Metal backed versus all-polyethylene unicompartmental knee arthroplasty: the effect of implant thickness on proximal tibial strain in an experimentally validated finite element model

Title Page

Metal backed *versus* all-polyethylene unicompartmental knee arthroplasty: proximal tibial strain in an experimentally validated finite element model

Ms Chloe E H Scott MSc FRCS(Tr&Orth) MD[1, 2] Specialist Registrar in Orthopaedics

Dr Mark J Eaton BEng PhD[3] Research Associate

Mr Frazer A Wade FRCSEd (Orth)[2] Consultant Orthopaedic Surgeon

Mr Richard W Nutton MD FRCS(Orth)[2] Consultant Orthopaedic Surgeon

Prof Sam L Evans BEng PhD[3] Professor of Engineering

Dr Pankaj Pankaj PhD[1] Reader in Numerical Modelling

[1]*Univeristy of Edinburgh, School of Engineering, Alexander Graham Bell Building, Mayfield Road, Edinburgh EH9 3JL*

[2]*Department of Orthopaedics, Royal Infirmary of Edinburgh, 51 Little France Crescent, Old Dalkeith Road, Edinburgh EH16 4SA*

[3] *Cardiff University, Institute of Mechanical and Manufacturing Engineering, Cardiff School of Engineering, Queen'sBuildings, The Parade, Cardiff CF24 3AA, UK.*

Metal backed *versus* all-polyethylene unicompartmental knee arthroplasty: proximal tibial strain in an experimentally validated finite element model

Abstract

Background: Up to 40% of unicompartmental knee arthroplasty (UKA) revisions are performed for unexplained pain which may be caused by elevated proximal tibial bone strain. This study investigates the effect of tibial component metal backing and polyethylene thickness on bone strain in a cemented fixed bearing medial UKA using a finite element model (FEM) validated experimentally by digital image correlation (DIC) and acoustic emission (AE).

Methods: Ten composite tibias implanted with all-polyethylene (AP) and metal backed (MB) tibial components were loaded to 2500N. Cortical strain was measured using DIC and cancellous microdamage using AE. FEMs were created and validated and polyethylene thickness was varied 6-10mm. The volume of cancellous bone exposed to <-3000 (pathological loading) and <-7000 (yield point) minimum principal (compressive) microstrain (με) and >3000 and >7000 με maximum principal (tensile) microstrain was computed.

Results: Experimental AE data and the FEM volume of cancellous bone with compressive strain <-3000με correlated strongly: R= 0.947, R^2 = 0.847, percentage error 12.5% ($p<0.001$). DIC and FEM data displayed correlation of 0.956. FEM strain patterns differed: MB lateral edge concentrations; AP concentrations at keel, peg and at the region of load application. Cancellous strains were higher in AP implants at all loads: 2.2 (10mm) to 3.2(6mm) times the volume of cancellous bone compressively strained <-7000με.

Conclusion: All-polyethylene tibial components display greater volumes of pathologically overstrained cancellous bone than metal backed implants of the same geometry. Increasing AP thickness does not overcome this and comes at the cost of greater bone resection.

Keywords: Unicompartmental knee arthroplasty; bone strain; finite element analysis

Article Summary

Article Focus:

- Experimental validation of a finite element model of medial UKA using acoustic emission data and digital image correlation.
- Investigation of the effect of UKA implant thickness and metal backing on cancellous bone strain.

Key Messages:

- All-polyethylene tibial components display greater proximal tibial cancellous bone strain than metal backed implants of the same geometry at physiological loads.
- Altering all-polyethylene component thickness markedly effects proximal tibial strain with thinner implants associated with greater strains.

Strengths and limitations of this study:

- Strengths of this FE study include experimental validation, the examination of bone strain and a novel investigation of metal backing in UKA.
- Limitations of this study include the use of composite tibiae, the performance of a linearly elastic analysis and the lack of kinematic analysis.

Introduction

Ten year survival of unicompartmental knee arthroplasty (UKA) varies from 80 to 96% between implants and institutions [1-3]. Unexplained pain is a leading cause of UKA failure: 24-48% of revisions across registries [1-3]. Elevated proximal tibial strain and microdamage may cause this pain [4, 5]. Joint registries do not distinguish between metal backed and all-polyethylene UKAs and there is a paucity of biomechanical evidence to inform decisions between implants of different material [6]. Finite element models (FEMs) of UKAs are few in number and most frequently analyse mobile bearing UKAs [4, 7-12]. The effect of implant thickness on proximal tibial strain has not been reported.

Orthopaedic FEMs are typically validated using strain gauge experiments. These measure strain only over the surface area to which they are attached. Acoustic emission can measure failure initiated inside a solid by detecting sound waves produced as material undergoes post-elastic deformation from plasticity or damage [13]. During plasticity, dislocation movement and cracking releases elastic waves of energy detectable on the material's surface by piezoelectric sensors in real time [13]. AE detected microdamage has been verified using micro-CT (μCT) [13]. To our knowledge AE has not previously been used to validate an FEM. Digital image correlation (DIC) is a non-destructive technique which measures surface strain. It involves observing with cameras the pattern of deformation on loading of a high-contrast speckle pattern applied to a surface. DIC has been used to measure macroscopic and microscopic surface strain in both cadaveric [14] and synthetic bone [15] and has been used previously to validate FEMs [16].

The aims of this study were:

- Validation of a finite element model of the proximal tibia implanted with cemented fixed bearing medial UKAs using experimental AE and DIC data [15].
- To investigate the effect of implant thickness and metal backing on cancellous bone strain.

We hypothesised that proximal tibial cancellous bone would experience greater strain under all-polyethylene tibial components than metal backed implants and that this would be exacerbated in thinner implants.

Materials and Methods

Mechanical Testing

Full details of the experimental methods can be found in Scott et al [15]. Ten 4th generation composite Sawbone tibias (model #3401, density Pcf(g/cc) 102 (1.64), Pacific Research Laboratories, Vashon, Washington, USA) were implanted with Sigma Partial (DePuy, Johnson & Johnson Professional Inc, Raynham, Massachusetts, USA) fixed bearing, non-conforming cemented medial UKA tibial components: 5 all-polyethylene (AP), 5 metal-backed (MB). The proximal tibia was coated with matt white paint and a black speckle pattern applied. Two charge-coupled DIC cameras (Limess, Messtechnik und Software GmbH, Krefeld, Germany) were positioned to view the anteromedial tibia. Implants were loaded using a servohydraulic machine (Losenhausen Maschinenbau, Dusseldorf) in 500N increments to a 2500N medial load. Cameras were calibrated and images taken at 500N increments. Images were 60mm wide giving a resultion of 0.0375mm/pixel. Strain in the vertical direction was measured at ≥80 consecutive points along an anteromedial line. DIC analysis was performed using Istra 4D 3.1 software (Dantec Dynamics, Skovlunde, Denmark). Acoustic emission (AE) hits were measured by two piezoelectric Pancom Pico-z AE sensors (125-750kHz, Pancom, Huntingdon, UK) and Mistras Group Ltd IL40S preamplifiers. AE recording was continuous and activity >45dB registered as a hit. Computer analysis was performed using AEWin 3.5 software.

Finite Element Model Creation and Validation

A CAD model of a 4th generation left composite tibia was obtained from the public domain (Biomed town) and imported into ABAQUS CAE Version 6.12 (Simulia, Dassault Systemes, Walthan, USA) as cortical and cancellous parts. Anatomical axes were defined in coronal and sagittal planes. The proximal tibia was cut perpendicular to the coronal anatomical axis at 6mm depth with 6° of posterior slope. The tibia was cut distally at 200mm below the intercondylar eminence to reduce computational effort.

CAD models of tibial components (size 3 MB tibia, 8mm tibial insert and a size 3 8mm AP tibia) and 1.5mm cement mantles were created using Autodesk Inventor 2012 (Autodesk Inc, San Rafael, CA, USA) based on implant measurements taken with a digital calliper sensitive to 1/100mm. These were imported into ABAQUS CAE Version 6.12 and assembled creating two models (figure 1):

1. Composite tibia with a cemented 8mm AP tibial component.

2. Composite tibia with a cemented MB tibial component and 8mm polyethylene insert.

All materials were assumed to be isotropic, homogenous, and linearly elastic. Material properties are shown in Table 1. *Linear tetrahedral meshes with a mean internodal distances of 1.5-2mm were used. Mesh resolution was based on a 2% convergence criterion for the displacement magnitudes in the proximal tibia* (Table 1). Cement was bonded to bone and tibial insert to metal baseplate using tie constraints. A coefficient of friction of 0.25 was used between implant and cement [17]. The distal tibia was fully constrained. Proximally the tibia was constrained against medial/lateral and anterior/posterior translations at a node representing the ACL footprint to prevent non-physiological bending.

Load was applied directly to the polyethylene articular surface. For validation purposes the medial plateau only was loaded (this refected the experimental set-up where the aim was to detect only microdamage originating medially): distributed load, uniform weighting, applied at the central node over a radius of 6mm (113.1mm^2 area). This closely reflected the contact area found experimentally of 116mm^2 [15] and the contact point reported in kinematic studies [18]. A 2500N load was applied parallel to the tibial mechanical axis. Strain data (volume of cancellous bone elements experiencing minimum principal strain <-3000 and <-7000με or maximum principal strain >3000 and >7000με, and peak minimum and maximum principal strains) were recorded at each 500N increment. In accordance with the commonly used convention in engineering, the negative sign denotes compression and positive tension.

To validate each FEM against AE mechanical testing data [15], the mean number of AE hits (>45dB) on loading and unloading 5 specimens of each implant were correlated with FEM predicted cancellous bone strain data. DIC measured minimal principal strain (vertical component) was correlated with FEM predicted cortical bone strain. Statistical analysis was performed using SPSS version 19.0 (SPSS Inc., Chicago, IL, USA). Correlation between parametric variables was assessed using Pearson's correlation coefficient. Linear regression analysis was used to explore significant correlations in continuous data with linear relationships. Autocorrelation was tested using the Durbin-Watson statistic (0 = positive autocorrelation, 4 = negative autocorrelation, 2 = no autocorrelation) and residuals were determined to be normally distributed prior to linear regression analysis.

After validation, additional FEM simulations were undertaken. CAD files were manipulated to create AP tibial components and MB polyethylene inserts of 6mm and 10mm thicknesses by adding or removing 2mm slices. To better represent physiological conditions, and eliminate bending from a unilateral load, a lateral plateau load was added as a distributed load at the central node with radius 6mm. A 60:40 medial:lateral load division [19] was used and a 4170N maximum total load applied (2500N medial load). This load is ~6 times body weight and reflects physiologic tibiofemoral loading [20]. Material properties, interactions, constraints and boundary conditions were unchanged. Numerical data was extracted for strain variables as before.

Results

FEM Validation

Compressive strain correlated with AE data more closely than tensile strain (Table 2). Greatest correlation existed between the volume of cancellous bone elements with compressive strain <-3000με and the number of AE hits on loading (Table 3, Figure 2). Anteromedial cortical bone minimal principal strain measured using DIC correlated strongly with that predicted by the FEM (Pearson's correlation AP: 0.956, p=0.01; MB: 0.885, p=0.01) (Figure 3).

Linear regression analysis results are shown in Table 3. Regression equations for both implants fitted the data significantly well (ANOVA of $p<0.005$). That is, the dependant outcome variable (AE hits on loading) was significantly predicted by the regression model using the independent FEM variables of volume of elements with strain >3000με or <-3000με.

For the MB implant, regression equations fitted well for all FE variables investigated (ANOVA $p<0.01$). For the AP implant, regression equations fitted well (ANOVA $p<0.05$) for volume of elements with compressive strain <-3000με. The equation for tensile strain >3000 με did not predict AE hits significantly well (ANOVA p=0.099). This is to be expected in a model loaded in compression.

Linear regression analysis was based on discrete AE hit data and FEM predicted strains. The strongest correlations existed for the MB implant (Table 3) ($p<0.008$ T-test). When data for both implants were combined, correlation was greatest between AE hits and FEM predicted volume of elements with compressive strain <-3000με (Table 3). AE measured microdamage and FEM predicted strains were related with a confidence of >95%.

Finite Element Analysis

Loading both plateaus altered the bone strain distribution for both implants: lateral strain shielding and medial metaphyseal flare strain concentrations (bending) were resolved.

Cancellous Bone Minimum Principal Strain

A greater volume of cancellous bone was strained below -3000 and -7000με in the 8mm AP than the 8mm MB model at every load (Figure 4). At lower loads (1668N and 2502N) twice the volume of cancellous bone had compressive strain of <-3000με in the AP than the MB implant. At 4170N the volume of elements with compressive strain <-7000με was three times greater in the AP implants (Figure 4).

Altering polyethylene thickness significantly affected the volume of overstrained cancellous bone in AP implants. At loads >2502N reducing AP implant thickness from 10 to 6mm increased the cancellous bone volume with compressive strain <-7000με by 1.5-3 times (Figure 4). Altering MB insert thickness made little difference to the volume of bone overstrained (Figures 4 and 5). AP implants displayed 2.2 (10mm) to 3.2 (6mm) times the volume of cancellous bone compressively overstrained <-7000με compared to MB implants at 4170N (Figure 4).

Strain contours demonstrated different patterns of minimum principal strain between implants (Figures 6 to 8). In the MB implant high compressive strain was confined to the cut tibial surface, but extended much deeper under the AP implant (Figures 6 and 7). In the AP implant, minimum principal strain was concentrated anteromedially in association with the keel and peg (Figure 7) and at the posteromedial rim of the tibia (Figure 7 and 8). Reducing

AP implant polyethylene thickness increased peg and keel concentrations (Figure 8). In the MB implant strain concentrated laterally at the implant corner and at the keel, with relative shielding at the peg (Figures 7 and 8). Altering MB insert thickness had little effect (Figure 8). Peak minimum principal and peak maximum principal strain occurred in elements just anterior to the implant keel in both implants.

Cancellous Bone Maximum Principal Strain

When loading in compression, tensile strains are the result of Poisson's effect. Therefore smaller volumes of cancellous bone experienced excessive tensile than compressive strains. The volume of cancellous bone with tensile strain >3000με differed significantly between implants at loads ≥2502N (Figure 5). Altering MB insert thickness made little difference to the volume of overstrained bone (Figure 5). Reducing AP thickness from 10 to 6mm increased the volume of cancellous bone with tensile strain >3000με by 1.5-3.24 times at loads ≥2502N (Figure 5). In 6mm implants, the ratio of cancellous bone volumes with tensile strain >3000με (AP:MB implants) was 5.7:1 at 2502N and 2.4:1 at 4170N. For 10 mm implants the ratios were 2.2:1 and 1.8:1 respectively.

The volume of cancellous bone with tensile strain >7000με differed between implants at high loads. At 4170N the volume of cancellous bone overstrained >7000με increased exponentially in the 6mm AP implant (Figure 5). Deformation was greater in AP implants with more bending in both coronal and sagittal planes.

Discussion

Cancellous bone strain differed significantly between AP and MB UKA implants with greater volumes of pathologically overstrained cancellous bone in AP implants and higher peak tensile strains. This concurs with mechanical testing [15] where AP implants displayed 1.8-6 times more microdamage (AE hits) than MB implants particularly at loads >1000N. Implant stiffness is a function of geometry and material properties. Large differences in the Young's moduli of polyethylene E=0.69GPa and cobalt-chrome E=210GPa [21] result in greater bending of the AP implant. Decreasing polyethylene thickness, and therefore stiffness, increased proximal tibial strain in the AP implant. Load distribution was more even in the MB implant which deformed less. The difference between implants was not overcome by

increasing AP thickness to 10mm. In MB implants, polyethyelene inserts of <8.5mm thickness have been associated with unacceptably high von Mises stresses [9], but there is currently no recommended minimum polyethylene thickness for UKA. The keel associated anteromedial strain concentration was more pronounced in the AP implant. Simpson et al [4] have reported a similar anteromedial von Mises strain concentration (140% that of an intact tibia) in the metal backed mobile bearing Oxford UKA (Biomet, Swindon, UK). This has been hypothesised as a source of unexplained anteromedial pain. The lateral corner strain concentration in the MB implant has been reported previously in the Oxford implant [4, 10]. This is the region with no cortical support and may reflect greater implant bending here than at cortically supported regions.

Joint registries do not distinguish between AP and MB UKA implants. Poor survivorship of AP UKAs has been reported [22-25] with early failures commonly due to tibial loosening, subsidence or pain. Whilst 10-15 year survival of 90-92% is reported for an AP implant with minimum thickness 9mm [26], components of 6mm have been associated with early clinical failure [27]and increased wear and osteolysis [28]. However, increasing AP implant thickness requires increased resection depth which reduces bone strength [29] and increases strain [4]. This may result in increased tibial component loosening or subsidence with thicker implants. Increasing AP thickness must therefore be balanced against larger bone resection. Actual minimum polyethylene thickness depends upon femoral component radius of curvature and bearing conformity: here 7.26mm (8mm AP implant) and 6.45mm (8mm MB insert).

It is argued that yielding and damage in bone is best described using strain rather than stress [30]. Strain based criteria are numerically more efficient and accurate than stress based criteria [30]. Previous UKA FEMs report von Mises stress and strains [7, 8, 12]. Gray et al [8] used 17 strain gauges to validate a composite tibia model (R^2=0.962, percentage error 5%) [8] and a cadaveric tibial model (R^2=0.98, percentage error 8.8%) [7] implanted with the Oxford UKA. Tuncer et al [11] used strain gauges to validate cadaveric tibia models with cemented (R^2=0.85) and uncemented (R^2=0.62) Oxford UKAs. Our correlation values between experimental AE data and predicted FEM data (Pearson's correlation 0.947, R^2 0.847, percentage error 12.5%) compare favourably. DIC is a recognised technique for FEM validation [16] and here has confirmed this validation.

The threshold limits of 3000 and 7000με were chosen to represent the strains at which cancellous bone is pathologically overloaded and fails, respectively [31]. The volume of elements in an FEM which can experience strains above or below threshold limits (e.g. 3000 or 7000με) is finite. As the volume of elements experiencing high strain increases, the volume available to experience high strains declines producing a sigmoid curve with a plateau region where further load increases cannot increase volume. This is very similar to what occurs in acoustic emission: when microfracture occurs with the emission of a hit, that region cannot emit further hits again producing a sigmoid curve. The consequence of these sigmoid curves is non-linear relationships when microdamage is greatest. At lower strain thresholds (eg. volume of elements with minimum strain <-3000με) the graphs for AP and MB implants converge as plateaus are approached. When the threshold is increased (to <-7000με) data shift to the linear region of the curve and differences between implants are more apparent. As MB implants remain in the linear region of the curve for the parameters measured, linear regression analyses give better predictive regression equations for MB than AP implants.

A linear elastic FEM was used in this study. Though bone is viscoelastic with non-linear behaviour, linear modelling can be used to reduce computing requirements when loading is not cyclical and not to failure [19, 30]. Experimental data support linear model use as the Felicity effect (AE activity occurring before the previous maximum applied load is reached, indicating permanent damage) was displayed by only one specimen at the loads applied.

Limitations of this study include the use of composite tibiae. These do not reflect the graduated trabecular structure of proximal tibial cancellous bone, but are applicable to the "average" tibia. Anisotropic, heterogeneous bone was modelled as isotropic and homogenous and a linearly elastic analysis was performed. This is a common method and does not discredit the differences found between implants. Gait was not modelled. As kinematic studies have shown the point of contact to change little throughout a range of motion in fixed bearing UKAs this was considered acceptable. The soft tissues of the intact lateral compartment were not modelled and this will have affected lateral strain.

This validated FEM study has shown UKAs with all-polyethylene tibial components to be associated with greater proximal tibial cancellous bone strain than metal backed implants of

the same geometry. These differences are present at physiological loads and increase at higher loads. Altering polyethylene thickness in metal backed implants has little effect on bone strain, but thinner polyethylene inserts display high internal strain, which may result in unfavourable wear characteristics similar to TKA [32, 33]. Altering all-polyethylene component thickness has marked effects on proximal tibial strain with thinner implants associated with greater strains. Increasing all-polyethylene implant thickness to 10mm does not overcome this difference and comes at the cost of greater bone resection.

Table 1. Material properties assigned to FEM parts [17, 21]. Cortical and cancellous bone properties apply to loading in compression.

Model	Part	Elastic Modulus (GPa)	Poissons ratio	Elements
AP	Cortical bone	16.7	0.3	105,375
	Cancellous bone	0.155	0.3	93,880
	PMMA Cement	2.4	0.3	19,691
	All-polyethylene tibia	0.69	0.46	23,950
MB	Cortical bone	16.7	0.3	105,375
	Cancellous bone	0.155	0.3	96,340
	PMMA Cement	2.4	0.3	6,371
	MB tibial tray (Co-Cr)	210	0.3	16,594
	Polyethylene insert	0.69	0.46	22,313

Table 2. Pearson's correlation of acoustic emission and finite element parameters. (*=p<0.01).

FE Parameter	AE Hits		
	Loading	Unloading	Total hits
Compressive Strain:			
Vol of elements <-3000με	0.947*	0.942*	0.970*
Vol of elements <-7000 με	0.802	0.854*	0.831*
Tensile Strain:			
Vol of elements >3000με	0.848*	0.914*	0.881*
Vol of elements >7000 με	0.540	0.699	0.581

Table 3. Linear regression analyses of AE hits (dependent variable) against FEM parameters (*x*: independent/predictive variables).

AE hits Vs:	R	R^2	SE of Estimate	DW	Linear Regression *y=a+bx*		SE of b	T score (p-value)	95% CI
					a	*b*			
Volume elements <-3000με compressive									
AP	0.917	0.840	19.6	3.49	4.12	0.009	0.002	3.98 (0.028)	0.002 to 0.015
MB	0.989	0.978	3.6	2.87	6.24	0.007	0.001	11.6 (0.001)	0.005 to 0.009
All	***0.947***	***0.847***	***12.6***	***3.3***	***4.27***	***0.008***	***0.001***	***8.37 (<0.001)***	***0.006 to 0.011***
Volume elements >3000με tensile									
AP	0.806	0.650	29.1	2.25	29.98	0.017	0.007	2.36 (0.099)	-0.006 to 0.04
MB	0.989	0.979	3.56	3.45	1.83	0.039	0.003	11.7 (0.001)	0.028 to 0.049
All	***0.848***	***0.720***	***20.8***	***1.8***	***18.2***	***0.02***	***0.004***	***4.5 (0.002)***	***0.01 to 0.031***

Acknowledgements

This research was supported by grants from the British Association for Surgery of the Knee, Joint Action (the orthopaedic research appeal of the British Orthopaedic Association) and the Engineering and Physical Sciences Research Council (EPSRC).

References

1. NJR. NJR of England and Wales: 9th Annual Report. In: Wales NEa, ed. 2012
2. Norwegian. Annual Report of the Norwegian Arthroplasty Register. In. 2010
3. Zealand N. New Zealand Orthopaedic Association: the New Zealand Joint Registry twelve year report. In. 2010
4. Simpson DJ, Price AJ, Gulati A, Murray DW, Gill HS. Elevated proximal tibial strains following unicompartmental knee replacement--a possible cause of pain. Medical engineering & physics 31(7): 752, 2009
5. Scott CE, Wade FA, Bhattacharya R, MacDonald D, Pankaj P, Nutton RW. Changes in Bone Density in Metal-Backed and All-Polyethylene Medial Unicompartmental Knee Arthroplasty. The Journal of arthroplasty, 2015
6. Small SR, Berend ME, Ritter MA, Buckley CA, Rogge RD. Metal backing significantly decreases tibial strains in a medial unicompartmental knee arthroplasty model. The Journal of arthroplasty 26(5): 777, 2011
7. Gray HA, Taddei F, Zavatsky AB, Cristofolini L, Gill HS. Experimental validation of a finite element model of a human cadaveric tibia. Journal of biomechanical engineering 130(3): 031016, 2008
8. Gray HA, Zavatsky AB, Taddei F, Cristofolini L, Gill HS. Experimental validation of a finite element model of a composite tibia. Proceedings of the Institution of Mechanical Engineers Part H, Journal of engineering in medicine 221(3): 315, 2007
9. Simpson DJ, Gray H, D'Lima D, Murray DW, Gill HS. The effect of bearing congruency, thickness and alignment on the stresses in unicompartmental knee replacements. Clinical biomechanics 23(9): 1148, 2008
10. Simpson DJ, Kendrick BJL, Dodd CAF, Price AJ, Gill HS, Murray DW. Load transfer in the proximal tibia following implantation with a unicompartmental knee replacement: a static snapshot. Proceedings of the Institution of Mechanical Engineers, Part H: Journal of Engineering in Medicine 225(5): 521, 2011
11. Tuncer M, Cobb JP, Hansen UN, Amis AA. Validation of multiple subject-specific finite element models of unicompartmental knee replacement. Medical engineering & physics 35(10): 1457, 2013
12. Kwon OR, Kang KT, Son J, Kwon SK, Jo SB, Suh DS, Choi YJ, Kim HJ, Koh YG. Biomechanical comparison of fixed- and mobile-bearing for unicomparmental knee arthroplasty using finite element analysis. Journal of orthopaedic research : official publication of the Orthopaedic Research Society 32(2): 338, 2014
13. Leung SY, New AM, Browne M. The use of complementary non-destructive evaluation methods to evaluate the integrity of the cement-bone interface. Proceedings of the Institution of Mechanical Engineers Part H, Journal of engineering in medicine 223(1): 75, 2009
14. Christen D, Levchuk A, Schori S, Schneider P, Boyd SK, Muller R. Deformable image registration and 3D strain mapping for the quantitative assessment of cortical bone microdamage. Journal of the mechanical behavior of biomedical materials 8: 184, 2012
15. Scott CE, Eaton MJ, Nutton RW, Wade FA, Pankaj P, Evans SL. Proximal tibial strain in medial unicompartmental knee replacements: A biomechanical study of implant design. The bone & joint journal 95-B(10): 1339, 2013
16. Ghosh R, Gupta S, Dickinson A, Browne M. Experimental validation of finite element models of intact and implanted composite hemipelvises using digital image correlation. Journal of biomechanical engineering 134(8): 081003, 2012
17. Completo A, Rego A, Fonseca F, Ramos A, Relvas C, Simoes JA. Biomechanical evaluation of proximal tibia behaviour with the use of femoral stems in revision TKA: an in vitro and finite element analysis. Clinical biomechanics 25(2): 159, 2010

18. Argenson JA, Komistek RD, Aubaniac JM, Dennis DA, Northcut EJ, Anderson DT, Agostini S. *In vivo* determination of knee kinematics for subjects implanted with unicompartmental arthroplasty. The Journal of arthroplasty 17(8): 1049, 2002
19. Conlisk N, Howie CR, Pankaj P. The role of complex clinical scenarios in the failure of modular components following revision total knee arthroplasty: A finite element study. Journal of orthopaedic research : official publication of the Orthopaedic Research Society, 2015
20. Kutzner I, Heinlein B, Graichen F, Bender A, Rohlmann A, Halder A, Beier A, Bergmann G. Loading of the knee joint during activities of daily living measured in vivo in five subjects. Journal of biomechanics 43(11): 2164, 2010
21. Callister WD, Rethwisch DG. Materials Science and Engineering. Asia: John Wiley and Sons, Inc., 2011
22. Furnes O, Espehaug B, Lie SA, Vollset SE, Engesaeter LB, Havelin LI. Failure mechanisms after unicompartmental and tricompartmental primary knee replacement with cement. The Journal of bone and joint surgery American volume 89(3): 519, 2007
23. Mariani EM, Bourne MH, Jackson RT, Jackson ST, Jones P. Early failure of unicompartmental knee arthroplasty. The Journal of arthroplasty 22(6 Suppl 2): 81, 2007
24. Hamilton WG, Collier MB, Tarabee E, McAuley JP, Engh CA, Jr., Engh GA. Incidence and reasons for reoperation after minimally invasive unicompartmental knee arthroplasty. The Journal of arthroplasty 21(6 Suppl 2): 98, 2006
25. Bhattacharya R, Scott CE, Morris HE, Wade F, Nutton RW. Survivorship and patient satisfaction of a fixed bearing unicompartmental knee arthroplasty incorporating an all-polyethylene tibial component. The Knee 19(4): 348, 2012
26. Newman J, Pydisetty RV, Ackroyd C. Unicompartmental or total knee replacement: the 15-year results of a prospective randomised controlled trial. The Journal of bone and joint surgery British volume 91-B: 52, 2009
27. Heck DA, Marmor L, Gibson A, Rougraff BT. Unicompartmental knee arthroplasty. A multicenter investigation with long-term follow-up evaluation. Clinical orthopaedics and related research (286): 154, 1993
28. Hernigou P, Poignard A, Filippini P, Zilber S. retrieved unicompartmental implants with full PE tibial compaonent: the effects of knee alignment and polyethylene thickness on creep and wear. Open Orthopaedics Journal 2: 51, 2008
29. Hvid I. Trabecular bone strength at the knee. Clinical orthopaedics and related research 227: 210, 1988
30. Pankaj P, Donaldson FE. Algorithms for a strain-based plasticity criterion for bone. International journal for numerical methods in biomedical engineering 29(1): 40, 2013
31. Frost HM. Strain and other mechanical influences on bone strength and maintenance. Curr OPin Orthop 8: 60, 1997
32. Bartel DL, Bicknell VL, Wright TM. The effect of conformity, thickness, and material on stresses in ultra-high molecular weight components for total joint replacement. The Journal of bone and joint surgery American volume 68(7): 1041, 1986
33. Pijls BG, Van der Linden-Van der Zwaag HM, Nelissen RG. Polyethylene thickness is a risk factor for wear necessitating insert exchange. International orthopaedics 36(6): 1175, 2012

Figures

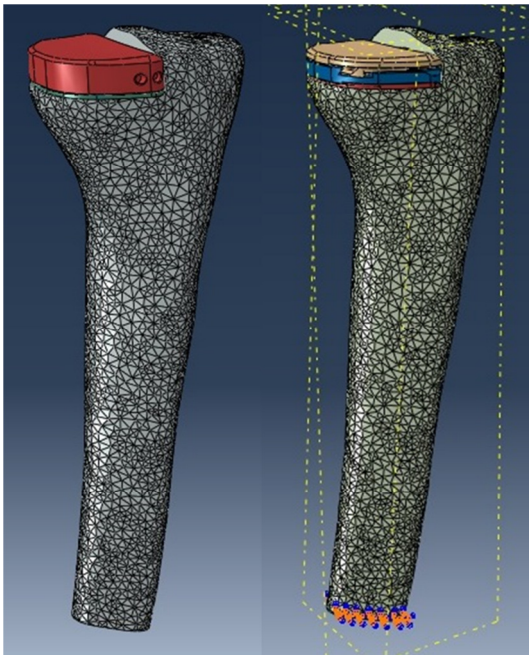

Figure 1. FEMs with 8mm AP implant (left) and 8mm MB implant (right). Datum planes indicate anatomical axes used as reference for implantation.

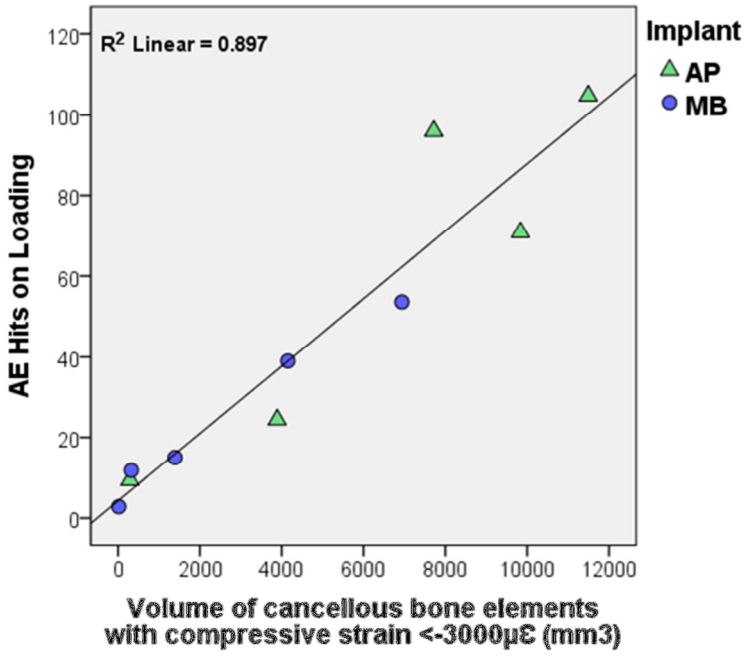

Figure 2. Scatter graphs for both implants showing the mean number of AE hits at each load compared to FEM predicted volume of cancellous bone elements with compressive (minimum principal) strain <-3000με.

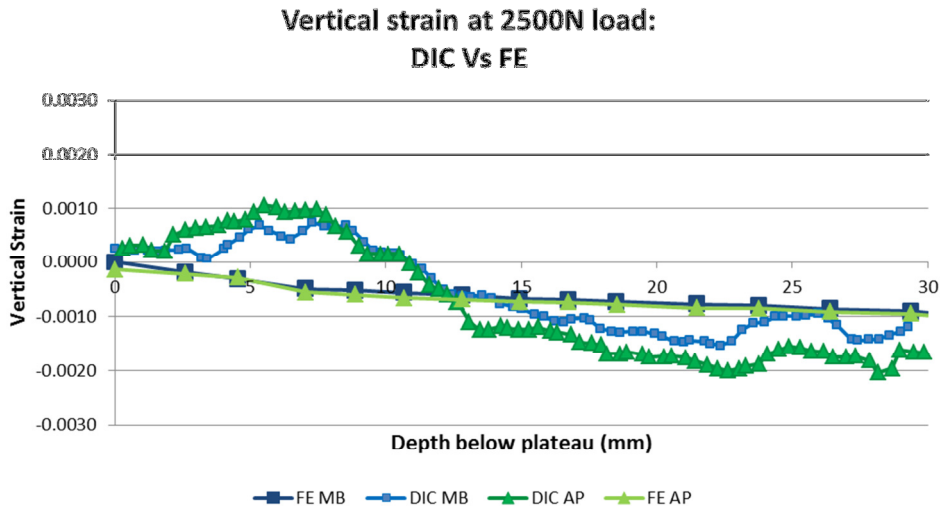

Figure 3. Cortical bone vertical strain along an anteromedial line for 8mm AP and MB implants: experimental DIC and predicted FEM data.

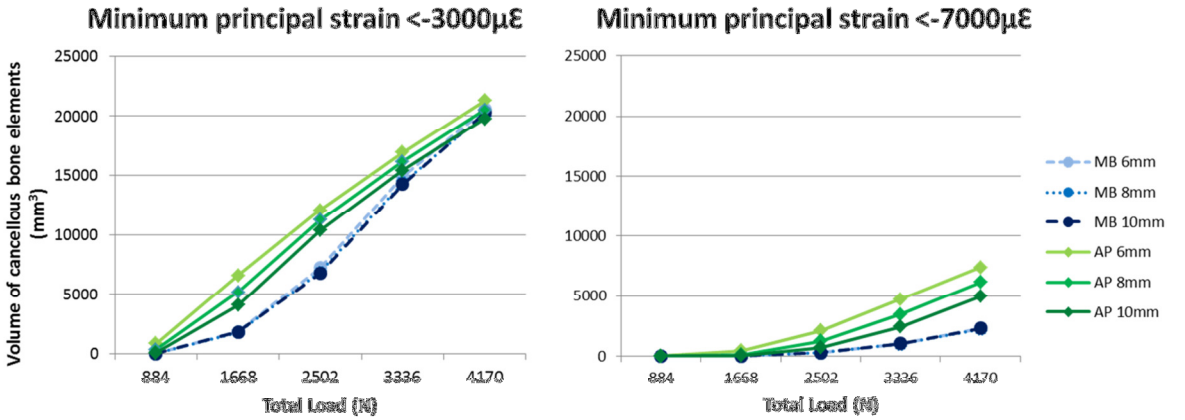

Figure 4. Volume of cancellous bone elements with compressive (minimum principal) strain <-3000με and <-7000με for both MB and AP implants of 6-10mm thickness.

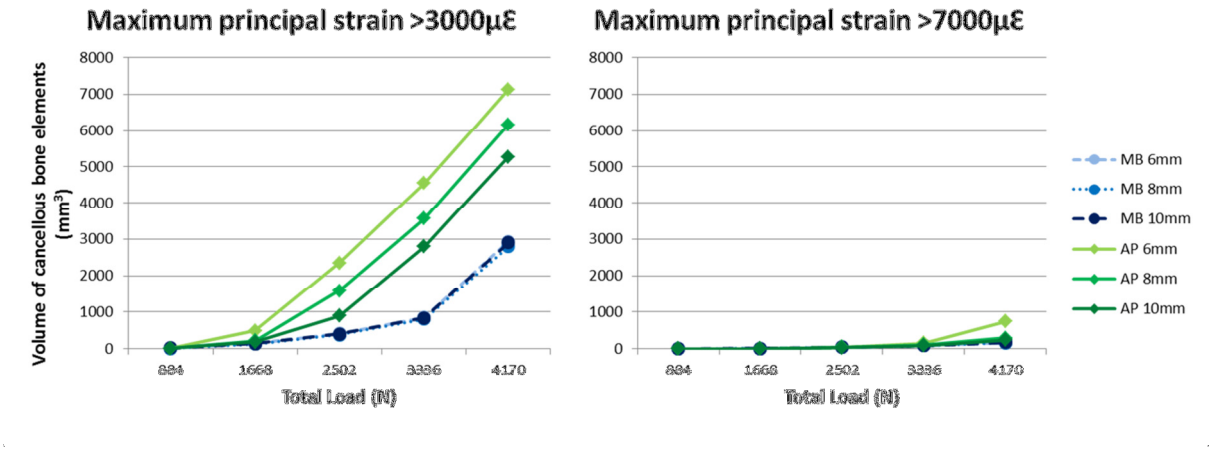

Figure 5. Volume of cancellous bone elements with tensile strain (maximum principal strain) >3000με and >7000με for both MB and AP implants of 6-10mm thickness.

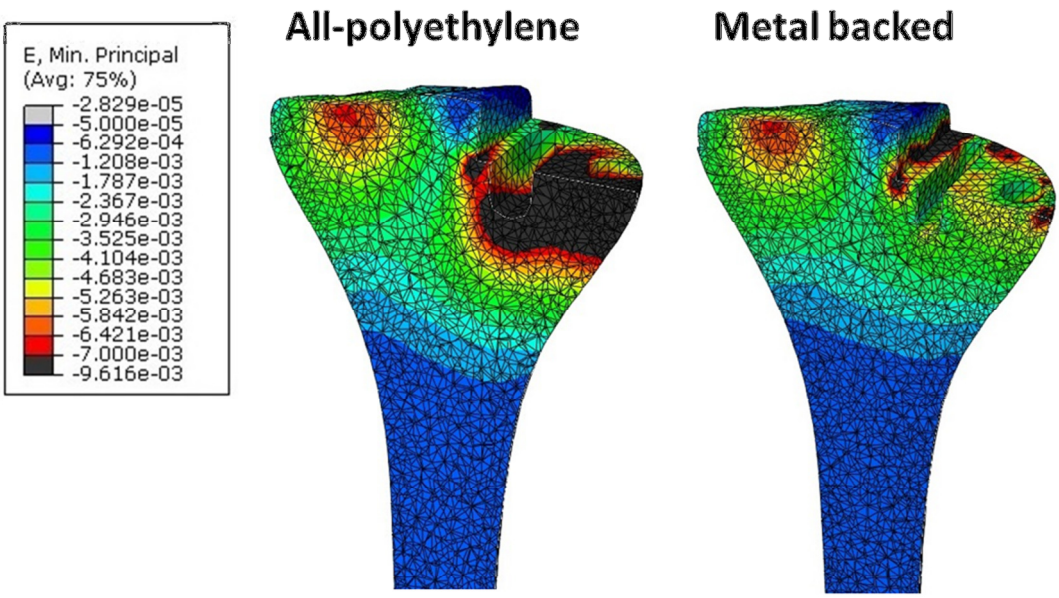

Figure 6. Mid-coronal oblique contours of the cancellous bone for each 8mm implant at total load of 4170N (medial load 2500N). Strain >-50με appears pale grey, strain <-7000με appears black.

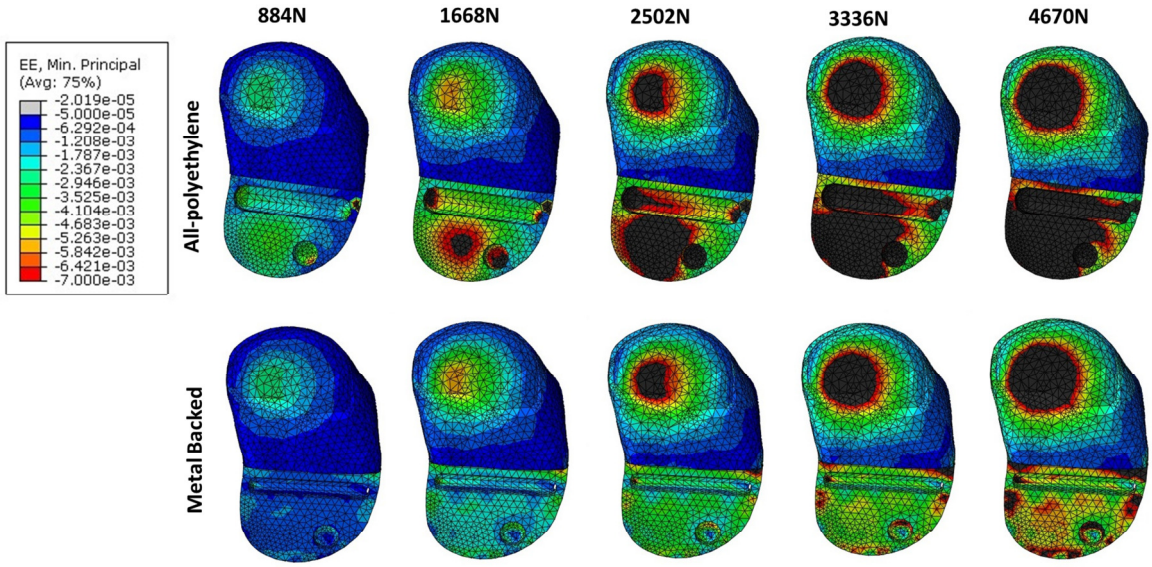

Figure 7. Medial aspect contour of the outer surface of cancellous bone for each 8mm implant. Strain >-50με appears pale grey, strain <-7000με appears black.

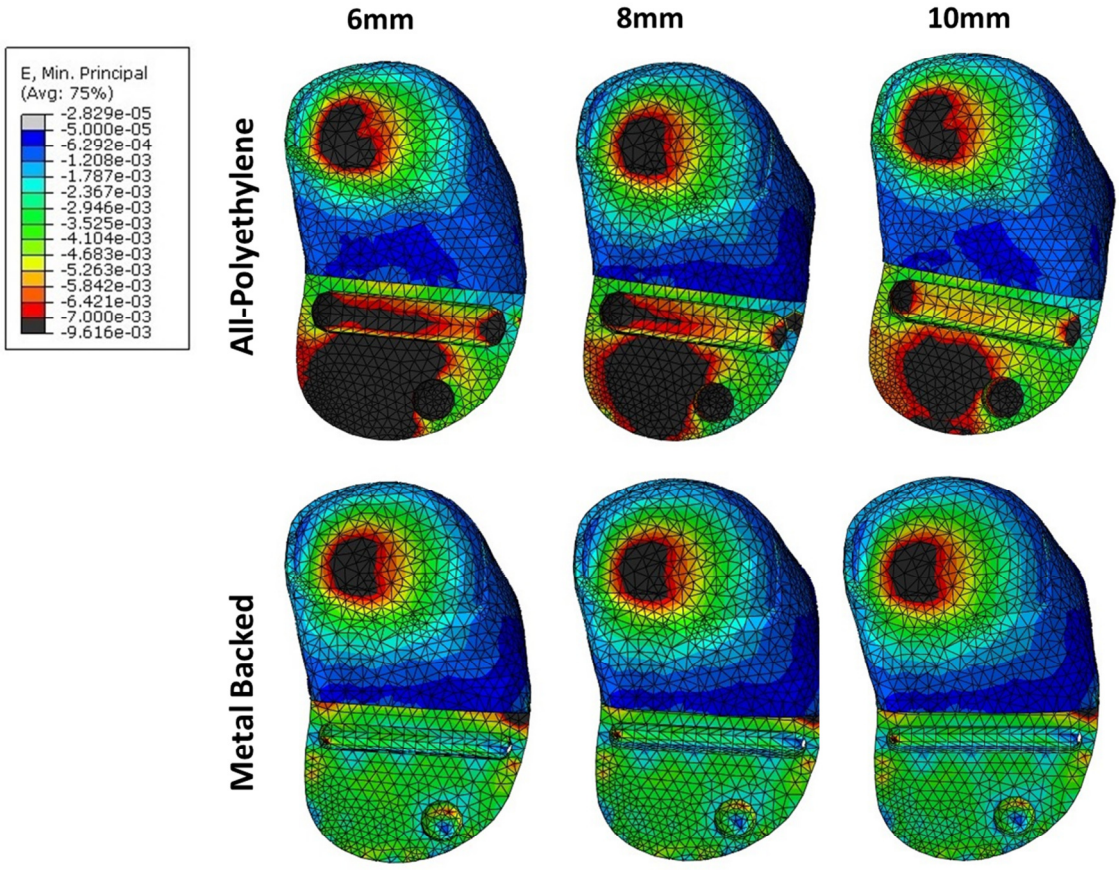

Figure 8. Axial compressive (minimum principal) contours of the upper surface of cancellous bone for implants of different thickness at a 2502N total load (1500N medial load). Strain >-50με appears pale grey, strain <-7000με appears black.

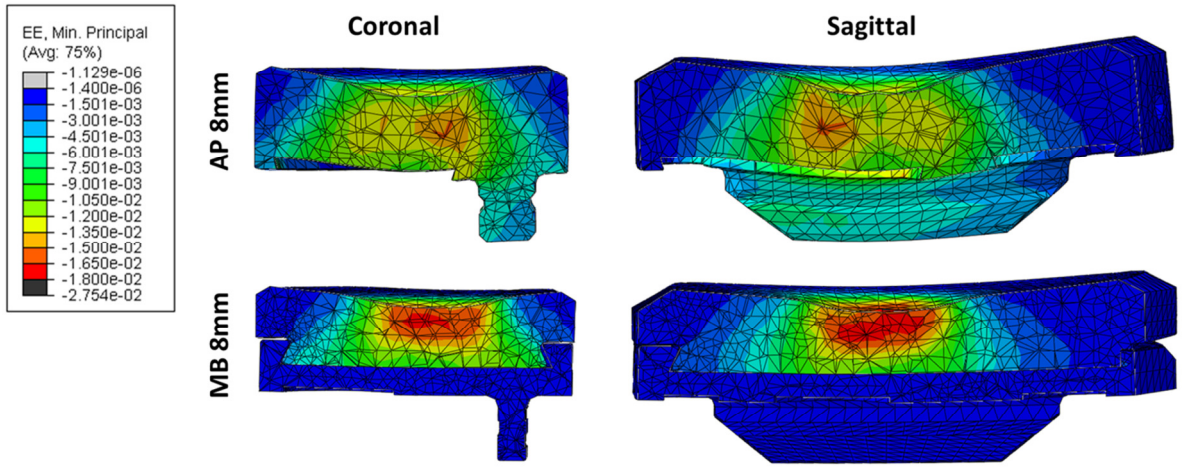

Figure 9. Coronal and sagittal plane contours showing implant deformation (x10) with a 2500N medial load.